



# Enantioseparation of $\beta^2$ -amino acids by liquid chromatography using core-shell chiral stationary phases based on teicoplanin and teicoplanin aglycone

Dániel Tanács<sup>a</sup>, Róbert Berkecz<sup>a</sup>, Aleksandra Misicka<sup>b</sup>, Dagmara Tymecka<sup>b</sup>, Ferenc Fülöp<sup>c</sup>, Daniel W. Armstrong<sup>d</sup>, István Ilisz<sup>a,\*</sup>, Antal Péter<sup>a</sup>

<sup>a</sup> Institute of Pharmaceutical Analysis, Interdisciplinary Excellence Centre, University of Szeged, Somogyi B. u. 4, H-6720 Szeged, Hungary

<sup>b</sup> Department of Chemistry, University of Warsaw, Pasteura str. 1, 02-093 Warsaw, Poland

<sup>c</sup> Institute of Pharmaceutical Chemistry, University of Szeged, Eötvös utca 6, H-6720 Szeged, Hungary

<sup>d</sup> Department of Chemistry and Biochemistry, University of Texas at Arlington, Arlington, TX 76019-0065, USA

## ARTICLE INFO

### Article history:

Received 30 April 2021

Revised 18 June 2021

Accepted 28 June 2021

Available online 5 July 2021

### Keywords:

$\beta^2$ -amino acids  
liquid chromatography  
macrocytic glycopeptide-based chiral stationary phases  
kinetic and thermodynamic characterization, core-shell particles

## ABSTRACT

Enantioseparation of nineteen  $\beta^2$ -amino acids has been performed by liquid chromatography on chiral stationary phases based on native teicoplanin and teicoplanin aglycone covalently bonded to 2.7  $\mu\text{m}$  superficially porous silica particles. Separations were carried out in unbuffered (water/methanol), buffered [aqueous triethylammonium acetate (TEAA)/methanol] reversed-phase (RP) mode, and in polar-ionic (TEAA containing acetonitrile/methanol) mobile phases. Effects of pH in the RP mode, acid and salt additives, as well as counter-ion concentrations on chromatographic parameters have been studied. The structure of selectands ( $\beta^2$ -amino acids possessing aliphatic or aromatic side chains) and selectors (native teicoplanin or teicoplanin aglycone) was found to have a considerable influence on separation performance. Analysis of van Deemter plots and determination of thermodynamic parameters were performed to further explore details of the separation performance.

© 2021 The Author(s). Published by Elsevier B.V.

This is an open access article under the CC BY license (<http://creativecommons.org/licenses/by/4.0/>)

## 1. Introduction

In the past decade, considerable interest has been paid to peptides containing  $\beta$ -amino acids ( $\beta$ -peptides). With an additional carbon atom between the amino and carboxylic groups, these  $\beta$ -amino acids can adopt various stable secondary structures with further functionalization possibilities enhancing the number of potential applications [1]. Unlike their analogs, these  $\beta$ -amino acids are not readily susceptible to hydrolysis or enzymatic degradation. Consequently, peptides with incorporated  $\beta$ -amino acids exhibit enhanced stability [2]. Additionally, chimeric peptides (mixed  $\alpha$ - and  $\beta$ -peptides) consisting of  $\alpha$ - and  $\beta$ -amino acids are of considerable interest as peptidomimetics in an increasing range of therapeutic applications [3,4]. Depending on the position of the side chain on the 3-aminoalkanoic acid skeleton  $\beta^2$ - and  $\beta^3$ -amino acids can be differentiated. The syntheses of  $\beta^2$ -amino acids in enantiomerically pure form are much more challenging than their  $\beta^3$ -

analogues [5]. The synthesis of  $\beta^2$ -amino acids in racemic form and their subsequent enantioseparation currently is the most practical and effective approach to obtain enantiopure  $\beta^2$ -amino acids. Chromatographic data related to the separation and identification of  $\beta^3$ -amino acid enantiomers have been reported in the literature [6–8]. However, relatively little information is available on the separation of  $\beta^2$ -amino acid enantiomers. The enantioseparation of a few  $\beta^2$ -amino acids have recently been carried out by direct high-performance liquid chromatography (HPLC) methods on chiral stationary phases (CSPs) based on (+)-(18-crown-6)-2,3,11,12-tetracarboxylic acid [9,10], macrocyclic glycopeptides [11,12], and *Cinchona* alkaloids [13,14].

Core-shell particles (superficially porous particles, SPPs) and sub-2  $\mu\text{m}$  fully porous particles (FPPs) are expected to provide high-throughput and effective separations of a variety of chiral molecules in ultra-high-performance liquid chromatography (UHPLC). Teicoplanin, teicoplanin aglycone, vancomycin, or isopropyl-cyclofructan covalently bonded to sub-2  $\mu\text{m}$  or 2.7  $\mu\text{m}$  SPPs were successfully applied for the enantioseparation of native and *N*-protected  $\alpha$ -amino acids and small peptides under LC [15–18], and supercritical fluid chromatography (SFC) conditions [19,20]. Te-

\* Corresponding author: István Ilisz, Institute of Pharmaceutical Analysis, University of Szeged, Somogyi B. u. 4, H-6720 Szeged, Hungary  
E-mail address: [ilisz.istvan@szte.hu](mailto:ilisz.istvan@szte.hu) (I. Ilisz).

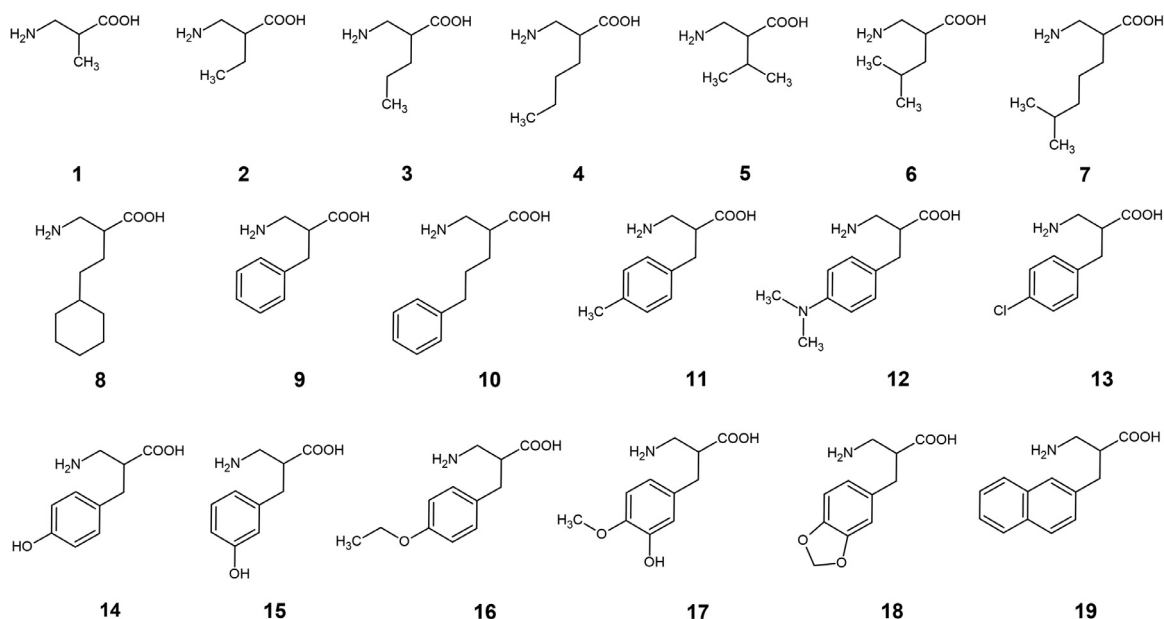


Figure 1. Structure of  $\beta^2$ -amino acids

icoplanin and teicoplanin aglycone covalently attached to 1.9  $\mu\text{m}$  FPP silica gel with narrow size distribution exhibited excellent separation performances for native proteinogenic amino acids in both LC and SFC modalities [21]. The new synthetic route developed for bonding teicoplanin to sub-2  $\mu\text{m}$  or 2.7  $\mu\text{m}$  SPPs and to sub-2  $\mu\text{m}$  FPPs endowed the selector with a zwitterionic character [22,23]. Ion-exchange-type CSPs are also being developed for UHPLC purposes. For example, *tert*-butylcarbamoyl(8 S,9 R)-quinine was covalently bonded to 1.9  $\mu\text{m}$  [22] or to 2.7  $\mu\text{m}$  [24–30] SPPs, and to 3.0  $\mu\text{m}$  and 1.7  $\mu\text{m}$  FPPs [28]. Lämmerhofer *et al.* [30] in chiral  $\times$  chiral two-dimensional UHPLC applied *tert*-butylcarbamoyl(8 S,9 R)-quinine and *tert*-butylcarbamoyl(8 R,9 S)-quinidine selectors bonded to 2.7  $\mu\text{m}$  SPPs for the separation of enantiomers of native proteinogenic  $\alpha$ -amino acids after peptide hydrolysis. A survey of literature data revealed that enantioseparations under UHPLC conditions were performed for proteinogenic  $\alpha$ -amino acids with the only exceptions being the enantioseparation of  $\gamma$ -aminobutyric acid [27] and  $\beta$ -Ala [28,34].

The present study provides results for the utilization of CSPs based on macrocyclic glycopeptides covalently bonded to 2.7  $\mu\text{m}$  SPPs for the enantioseparation of 19 unusual  $\beta^2$ -amino acids. Experiments were performed utilizing columns with 3.0 and 2.1 mm internal diameter (i.d.) based on teicoplanin- and teicoplanin aglycone. RP and polar-ionic mobile phases were applied in separations. Effects of the nature and concentration of the mobile phase components, acid and salt additives under various conditions, and pH in reversed-phase (RP) mode were studied. To gain detailed information about the chiral recognition process, structure–retention (selectivity) relationships were evaluated by taking into account the structural features of both the analytes and selectors. Analysis of van Deemter plots served as a basis for the kinetic investigations, while the temperature dependence study allowed thermodynamic characterization. In a few cases, elution sequences also were determined.

## 2. Experimental

### 2.1. Chemicals and materials

Nineteen racemic amino acids (1–19) were synthesized as described earlier [13]. (For structures see Fig. 1). Enantiomers (*R*)-2,

(*S*)-5 and (*S*)-6 were generous gifts from Prof. D. Tourwé (Vrije Universiteit Brussels, Brussels, Belgium).

Methanol (MeOH), acetonitrile (MeCN), and water of LC-MS grade,  $\text{NH}_3$  dissolved in MeOH, triethylamine (TEA), formic acid (FA), glacial acetic acid (AcOH), ammonium formate ( $\text{HCO}_2\text{NH}_4$ ), and ammonium acetate ( $\text{NH}_4\text{OAc}$ ) of analytical reagent grade were from VWR International (Radnor, PA, USA). The pH reported for the reversed-phase mobile phase is the apparent pH ( $\text{pH}_a$ ), which was adjusted directly in the aqueous triethylammonium acetate (TEAA)/MeOH solutions with the addition of AcOH.

### 2.2. Apparatus and chromatography

LC measurements were carried out on a Waters® ACQUITY UPLC® H-Class PLUS System with Empower 3 software (Waters) and components as follows: quaternary solvent manager, sample manager FTN-H, column manager, PDA detector, and QDa mass spectrometer detector. The parameters for the QDa detector were set as follows: positive ion mode, probe temperature, 600 °C, capillary voltage, 1.5 V, cone voltage, 20 V.

Chiral columns, based on teicoplanin (TeicoShell, **T**) and teicoplanin aglycone (TagShell, **TAG**) attached covalently to the surface of 2.7  $\mu\text{m}$  SPPs, were applied in this study. The core diameter and shell thickness of the SPPs were 1.7  $\mu\text{m}$  and 0.5  $\mu\text{m}$ , respectively. All columns (AZYP, LLC, Arlington, TX, USA) have 100  $\times$  3.0 mm i.d. or 100  $\times$  2.1 mm i.d. dimensions (abbreviations for columns: **T-3.0** and **T-2.1**; **Tag-3.0** and **Tag-2.1**).

Stock solutions of analytes (1–10  $\text{mg ml}^{-1}$ ) were prepared in MeOH and diluted with the mobile phase. The dead-time ( $t_0$ ) of the columns was determined by 0.1% AcOH dissolved in MeOH and detected at 210 or 256 nm. In all experiments a flow rate of 0.3  $\text{ml min}^{-1}$  provided efficiency and fast analysis for both column dimensions, while the column temperature was set at 20 °C (if not otherwise stated).

## 3. Results and discussion

Based on their side chain, the investigated  $\beta^2$ -amino acids can be divided into two sub-groups: those that contain an aliphatic moiety or an aromatic moiety. The branch or the length of the aliphatic moiety or the nature and position of substituents on the

aromatic ring influences the size and polarity of the molecule and is expected to have a considerable effect on selector-analyte interactions.

### 3.1. Effect of pH on retention and separation performance

The pK value of carboxylic groups of teicoplanin and teicoplanin aglycone (playing important role in the retention mechanism) is approximately 2.5. The pK values of the amino groups of  $\beta^2$ -amino acids **1-19** are in the range 10.16–10.32. The corresponding values for the carboxylic moieties of **1-12**, **19** are between 4.10–4.50, whereas for **13-18** they are between 3.20–3.60 (calculated with Marvin Sketch v. 17.28 software, ChemAxon Ltd., Budapest). Therefore, the charge of macrocyclic glycopeptide-based stationary phases and analytes is sensitive to pH and alters the interactions between the CSP and the analyte. To reveal the possible effects of  $pH_a$  on retention, selectivity, and resolution of  $\beta^2$ -amino acids bearing aliphatic (**3**) and aromatic side chain (**9**) were selected and their retention behavior was investigated on **T-3.0** and **TAG-3.0** columns in the RP mode applying eluents consisting of *aq*.TEAA/MeOH (90/10 v/v and 30/70 v/v) with a constant TEAA concentration of 20.0 mM and varying  $pH_a$  of the mobile phase between  $pH_a$  3.5–6.5. Under the studied conditions, the retention factors of the first eluting enantiomer ( $k_1$ ) usually changed slightly with increasing  $pH_a$  for both analytes, and only analyte **9** exhibited moderate increases in the *aq*.TEAA/MeOH 30/70 (v/v) eluent (Fig. S1). Interestingly,  $\alpha$  and  $R_S$  increased more significantly in both mobile phase systems, especially for analyte **3**, with the highest values obtained above  $pH_a$  5.0 (Fig. S1). Based on their pK values, teicoplanin, teicoplanin aglycone, and  $\beta^2$ -amino acids are present in ionized form under these mobile phase conditions. That is, the observed behavior is probably due to increased ionic interactions between the protonated amino group of the analyte and the deprotonated carboxylic group of the selector. The ionic structures affect either directly the Coulombic or dipolar interactions between the analyte and selector, or influence indirectly the retention by changing the conformation of the macrocyclic glycopeptides. To obtain the highest resolution and selectivity an eluent  $pH_a$  of 5.0 or above can be recommended for the enantioseparation of  $\beta$ -amino acids.

### 3.2. Effects of mobile phase composition on the chromatographic performance

Employing analytes **3** and **9**, first, the effects of five different mobile phase additives (salts or acids, namely  $HCO_2NH_4$ ,  $NH_4OAc$ , TEAA, FA, and AcOH) were studied on the chromatographic performance of **T-3.0** and **TAG-3.0** CSPs. Experiments were performed with a constant aqueous to organic solvent ratio ( $H_2O/MeOH$  90/10 v/v) and a constant additive concentration (20.0 mM, calculated for the whole eluent system). In the case of organic salts, the  $pH_a$  was adjusted to 5.0 by the addition of the corresponding acid. Mobile phases containing solely 20.0 mM FA or AcOH (without pH adjustment) resulted in unresolved peaks with rather poor peak shapes (Fig. S2). In contrast, when  $HCO_2NH_4$ ,  $NH_4OAc$  or TEAA were used as mobile phase additive, resolution could be obtained. Employing TEAA has led to symmetrical peak shapes, very good efficiencies, and selectivities. Therefore, in further experiments, TEAA was the favored mobile phase additive. It is worth mentioning that regarding MS-based detection,  $NH_4OAc$  offers higher sensitivity with acceptable peak shapes and resolution.

MeOH and MeCN organic modifiers are used commonly in amino acid separations [9]. The nature and concentration of the mobile phase components can exert considerable effects on retention and separation. Therefore, we next investigated the effects of organic modifiers on the enantioseparation of analytes **3**

and **9** utilizing **T-3.0** and **TAG-3.0** CSPs. Figure 2 shows the chromatographic figures of merit for the separations of analytes **3** and **9** in three different eluent systems. In unbuffered RP mode (a), mobile phase compositions of  $H_2O/MeOH$  90/10–10/90 (v/v), in buffered RP mode (b), *aq*.TEAA/MeOH 90/10–30/70 (v/v) containing 20 mM TEAA and  $pH_a$  5.0, and in polar-ionic mode (c), MeCN/MeOH 90/10–10/90 (v/v) containing 20 mM TEAA were applied.

In the unbuffered eluent system (Fig. 2 A),  $k_1$  increases with increasing MeOH content, however, not in the whole range studied. The observed phenomenon is at least partly for the lower solubility of amino acids with polar character in the less polar MeOH. The observed minimum in the curve for analyte **9** indicates an increased hydrophobic interaction at higher water content. Regarding  $\alpha$  and  $R_S$  values, they increase with increasing MeOH content. Interestingly, comparing the two CSPs,  $k_1$  values were higher on the **T-3.0** column, while higher  $\alpha$  and  $R_S$  values were registered on **TAG-3.0**, which may indicate reduced nonselective interactions in the latter case.

Under buffered RP conditions (Fig. 2B), similar to the unbuffered eluents, a slight increase in  $k_1$ ,  $\alpha$ , and  $R_S$  values was registered with increasing MeOH content. As an exception, analyte **9** on the **TAG-3.0** column first showed a moderate increase, then a slight decrease for  $k_1$ . Comparing these two eluent systems, a remarkable difference between chromatographic performances can be noted. In the presence of TEAA, higher  $\alpha$  and  $R_S$  values are obtained with significantly lower retentions, suggesting a pronounced suppression of nonselective interactions between the analytes and the stationary phase by the salt addition.

The results obtained with the application of mixtures of MeCN and MeOH along with acid and base additives in the polar-ionic mode are depicted in Fig. 2 C. With variation in the composition of the eluent the acid-base equilibrium and proton activity will be changed. At high MeCN content, the solvation of polar amino acids in the aprotic solvent decreases resulting in high retentions, while the increasing ratio of protic MeOH favors the solvation of polar amino acids, i.e., retention decreases. The change of  $\alpha$  and  $R_S$  values exhibited trends similar to those discussed above. The improved selectivity with increasing MeOH content suggests that hydrogen bonding may not play a major role in these enantioseparations.

### 3.3. Effects of the counter-ion concentration

The stoichiometric displacement model [31] is applied frequently to describe the retention behavior based on ion-pairing and ion-exchange mechanisms, predicting a linear relationship between the logarithm of the retention factor and the logarithm of the counter-ion concentration,

$$\log k = \log K_z - Z \log c_{\text{counter-ion}} \quad (1)$$

where  $Z$  is the ratio of the number of charges of the cation and the counter-ion, while  $K_z$  describes the ion-exchange equilibrium. If an ion-exchange mechanism exists, plotting  $\log k$  against  $\log c_{\text{counter-ion}}$  will result in a straight line with a slope proportional to the effective charge during the ion-exchange process, while the intercept provides information about the equilibrium constant.

To probe the potency of the simple displacement model in our case, experiments were carried out on **T-3.0** and **TAG-3.0** CSPs applying mobile phases b, *aq*.TEAA/MeOH (90/10 v/v,  $pH_a \approx 5.5$ ) and c, MeCN/MeOH (10/90 v/v) both containing 5.0–160 mM TEAA. In a cation exchange process in the presence of TEAA, the protonated triethylammonium ion acts as a competitor. The results presented in Fig. 3, definitely indicate the applicability of the stoichiometric displacement model, i.e., they support the involvement of ion-interaction processes in the retention mechanism. In

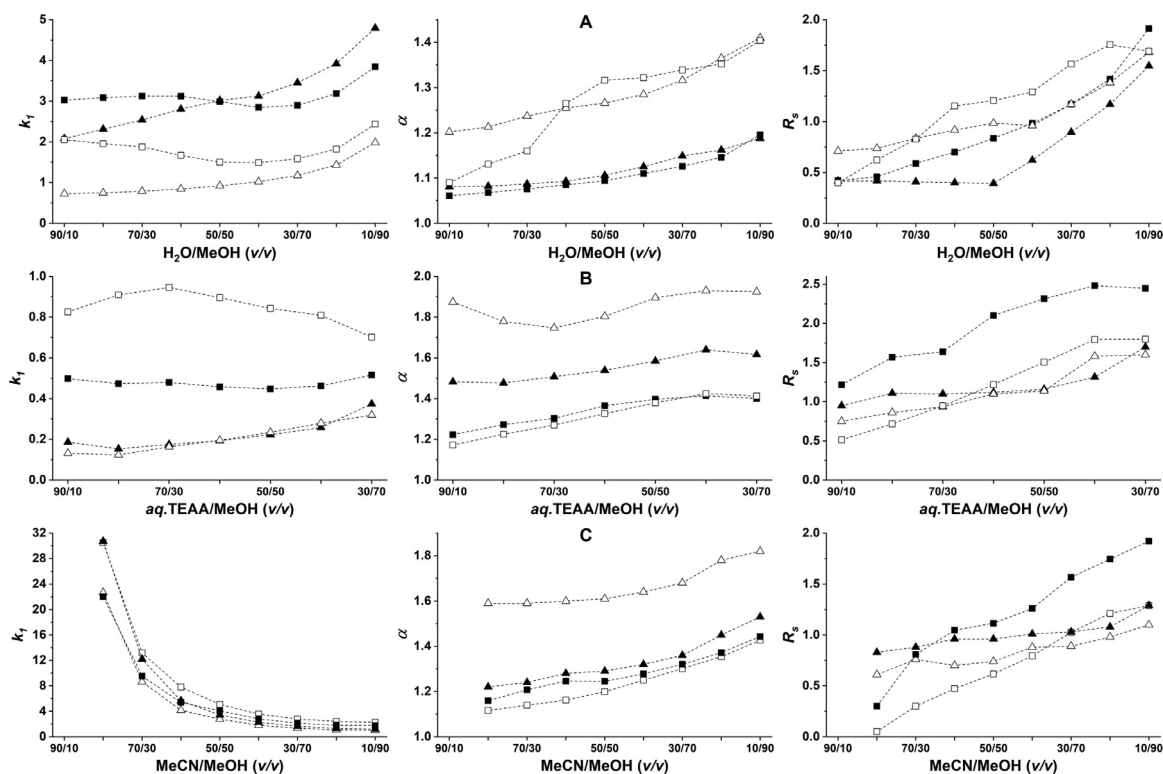


**Figure 2.** Effect of bulk solvent composition on chromatographic parameters for analyte **3** and **9** applying different mobile phase systems. Chromatographic conditions: column, T-3.0 and TAG-3.0; mobile phase, **a**, H<sub>2</sub>O/MeOH (90/10–10/90 v/v), **b**, aq.TEAA/MeOH (90/10–30/70 v/v), concentration of TEAA in mobile phase 20.0 mM and the actual pH of the mobile phase, pH<sub>a</sub> 5.0, **c**, MeOH/MeCN (90/10–10/90 v/v), concentration of TEAA in mobile phase, 20.0 mM; flow rate, 0.3 ml min<sup>-1</sup>; detection, 210–258 nm; temperature, 20 °C; symbols, on T-3.0 for analyte **3**, ▲, for analyte **9**, ■, on TAG-3.0 for analyte **3**, △, for analyte **9**, □

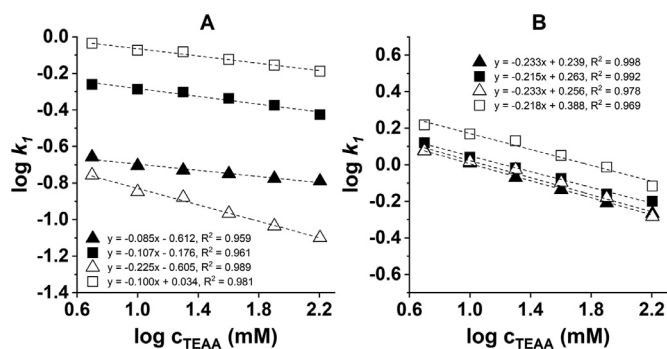


**Figure 3.** Effect of ion content on retention factor of the first eluting enantiomer,  $k_1$  for analytes **3** and **9**. Chromatographic conditions: column, T-3.0 and TAG-3.0; mobile phase, **A**, aq.TEAA/MeOH (90/10 v/v), concentration of TEAA in mobile phase, 5.0–160 mM, **B**, MeCN/MeOH (10/90 v/v), concentration of TEAA in mobile phase, 5.0–160 mM; flow rate, 0.3 ml min<sup>-1</sup>; detection, 210–258 nm; temperature, 20 °C; symbols, on T-3.0 for analyte **3**, ▲, for analyte **9**, ■, on TAG-3.0 for analyte **3**, △, for analyte **9**, □

this study, linear relationships were found between  $\log k_1$  vs.  $\log c_{\text{counter-ion}}$ , with slopes varying between about (–0.10) and (–0.23). In an earlier study, slopes around –1.0 were found for strong ion-exchangers, where the selector and selectand act in almost fully ionized form [32]. In absolute terms, the smaller slopes observed reveal a marked difference between the strong and weak ion-exchanger-based CSPs [33]. In the case of weak ion-exchanger CSPs, the retention (affected by the pH and the ionic state of the selector and analyte) can be reduced with the enhancement of the counterion concentration, but only to a limited range. It is worth mentioning that on both CSPs, practically equal slopes were calculated for each enantiomer, i.e., no significant difference could be observed

in the enantioselectivities with varying counter-ion concentration (data not shown).

### 3.4. Effects of structures of selector and analyte on retention and selectivity

The structure of both the chiral selector and the analyte affects considerably their interactions resulting in different retention and separation characteristics. To gain a set of chromatographic data, screening of the enantioseparation of 19  $\beta^2$ -amino acids was performed on four teicoplanin and teicoplanin aglycone-based columns in three different mobile phase systems: unbuffered RP (**a**, H<sub>2</sub>O/MeOH 30/70 v/v), buffered RP (**b**, aq.TEAA/MeOH 30/70 v/v, containing 2.5 mM TEA and 5.0 mM AcOH, pH<sub>a</sub> 5.5), and a polar-ionic mobile phase (**c**, MeCN/MeOH 30/70 v/v, containing 2.5 mM TEA and 5.0 mM AcOH). The related chromatographic data are summarized in Tables S1–S4. All studied  $\beta^2$ -amino acids were baseline-separated on at least one CSP, and often with both CSPs within three to five minutes depending on the nature of analytes, mobile phase, and inner diameter of columns. The overall success rate of the enantioseparations is depicted in Fig. S3. Taking into account the time needed for the analyses, application of mobile phase **a** and **b** seemed to be more favorable (Tables S1–S4). It should be noted, that the analysis time obtained here is three to ten times lower than that observed earlier on 5  $\mu\text{m}$  particles and 4.6 mm i.d. columns [10–13]. It was also observed that, in most cases,  $\beta^2$ -amino acids possessing aliphatic side chains (analytes **1–8**) exhibited slightly smaller  $R_S$  values than analytes with aromatic side chains (**9–19**). This is in spite of their similar enantioselectivity ( $1.30 < \alpha < 2.20$ ). For analytes **9–19**, in almost all cases,  $R_S > 1.5$  was obtained on all four columns applied with any of the three mobile phase systems (exceptions were compounds **12** and **13**).

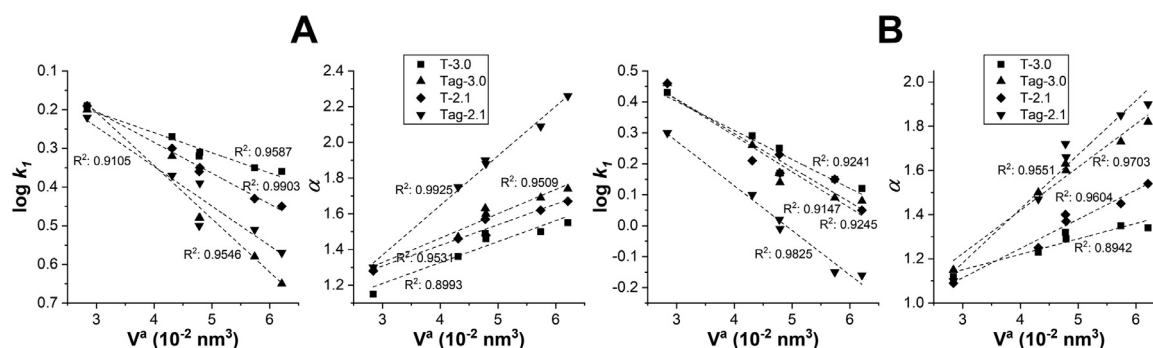


**Figure 4.** Dependence of retention factors of the first eluting enantiomer ( $k_1$ ) and separation factors ( $\alpha$ ) of analytes **1-6** on the Meyer substituent parameter ( $V^a$ ) Chromatographic conditions, column, T-3.0, T-2.1, TAG-3.0 and TAG-2.1; mobile phase, **A**, aq. TEAA/MeOH (30/70 v/v), concentration of TEA and AcOH in mobile phase 2.5 and 5.0 mM, respectively and the actual pH of the mobile phase, pH<sub>a</sub> 5.5, **B**, MeCN/MeOH (30/70 v/v), concentration of TEA and AcOH in mobile phase 2.5 and 5.0 mM, respectively; flow rate, 0.3 ml min<sup>-1</sup>; detection, 210–258 nm; temperature, 20 °C; symbols, for T-3.0 ■, for TAG-3.0 ▲, for T-2.1 ◆ and for TAG-2.1 ▼

In order to determine the specific structural effects of analytes possessing alkyl side chains on chromatographic data such as  $k_1$  and  $\alpha$ , the effect of the volume of the alkyl substituents ( $V^a$ ) was investigated. The steric effect of a substituent on the reaction rate can be characterized by the size descriptor of the molecule,  $V^a$  [34]. The  $V^a$  values for Me, Et, Pr, Bu, 2-Pr, and 2-Bu moieties are 2.84, 4.31, 4.78, 4.79, 5.74, and  $6.21 \times 10^{-2}$  nm<sup>3</sup>, respectively. Note, that there are no  $V^a$  values available for 6-methylheptanoic (**7**) and 5-cyclohexylpentanoic (**8**) moieties. Values of  $k_1$  and  $\alpha$  showed a good correlation with  $V^a$  on all studied columns in all three eluent systems. As the data presented in Fig. 4 confirm the volume of the alkyl substituents markedly influenced  $k_1$ : a bulkier substituent hindered the interactions between the selector and analyte leading to reduced retention. Since the difference in the interactions of the two enantiomeric analytes with the CSP differed considerably, an enhanced chiral recognition with higher  $V^a$  values could be observed. It should be noted here, that not only the position and bulkiness of the substituent but also the steric effect may heavily influence retention behavior and chiral recognition of  $\beta^2$ -amino acids.

Comparing the separation of analytes **9-19** possessing aromatic or substituted aromatic side chains to analytes **1-8**, shows higher  $R_S$  values for analytes **9-19**. In most cases, the  $R_S$  was above 1.5 and only analytes **12** and **13** exhibited poorer resolution (Table S1–S4). The most relevant and optimized data of separations are depicted in Table 1. The presence of an aromatic moiety instead of an aliphatic side chain in **9-19** probably improves  $\pi$ - $\pi$ -interactions between the enantiomers and the chiral selector and contributes to better chiral recognition. Enantiomers of analyte **12** possessing an additional 4-dimethylamino moiety (pK<sub>a</sub> 5.0, calculated with Marvin Sketch v. 17.28 software, ChemAxon Ltd., Budapest) were baseline-separated only in mobile phases **b** and **c**, where the ionic strength could be kept at a constant level.

Analytes **11**, **13**, and **14** possess a methyl, chlorine, or hydroxyl substituent at position 4 of the aromatic ring, giving  $\pi$ -basic or  $\pi$ -acidic character to the molecules. Figures 5 and S4 are chromatograms that illustrate the separation performance obtained on TAG-3.0 and T-3.0 CSPs in two different eluent systems. The methyl and chlorine moieties show slight effects on retention, selectivity, and resolution, while the hydroxyl moieties and their positions in analytes **14** vs. **15** affect considerably the separation performance. The 3-position of the hydroxyl moiety probably favors steric interactions between selector and analyte resulting in higher selectivity and resolution, in particular, on the TAG-3 CSP in H<sub>2</sub>O/MeOH (30/70 v/v) mobile phase (Fig. 5 A). These differences, especially in resolution, can be observed in Fig. S4 A and S4B.

Analytes **16-18** possess an additional ether O-atom, which is capable of H-bond interactions, while **19** bears a naphthyl moiety,

which may facilitate stronger  $\pi$ - $\pi$ -interactions. All these structural features led to higher  $\alpha$  and  $R_S$  values as depicted in Fig. 5B and Fig. S4B.

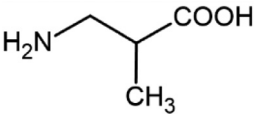
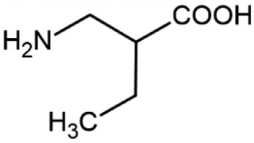
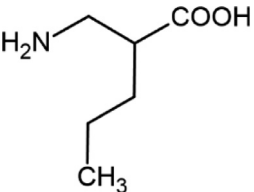
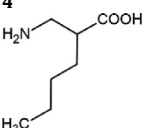
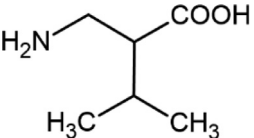
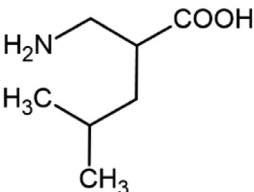
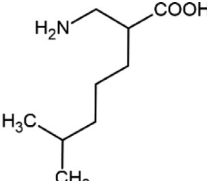
In addition to the chromatograms for analytes **11-19**, Figure 6 depicts selected chromatograms for analytes **1-10** and **12** as well representing the separations obtained within three minutes. Using enantiopure analytes, elution sequences for analytes **2**, **5**, and **6** were determined and found to be the same for all columns and mobile phases, they were,  $R < S$ .

According to the data in Tables S1–S4, the separation factors, despite similar retention times and retention factors of the first eluting enantiomers, sometimes differ considerably on the teicoplanin- and teicoplanin aglycone-based CSPs, indicating a possible difference in the separation mechanism. In most cases, higher selectivities and resolutions were obtained with the aglycone-based CSP under all the studied conditions, while no clear trend could be observed for the variation in the retention times. As described earlier [35] the sugar units of the native teicoplanin may affect the chiral recognition process in different ways; they block the possible interaction sites on the aglycone, occupy the space inside the “basket”, and offer additional interaction sites since the three sugar units are themselves chiral. To quantitatively determine the effects of the sugar units, the equation  $\Delta(\Delta G^\circ) = -RT \ln \alpha$  was applied for the calculation of the differences in enantioselective free energies between the two CSPs [ $\Delta(\Delta G^\circ)_{TAG} - \Delta(\Delta G^\circ)_T$ ]. As illustrated in Fig. 7, the energy differences [ $\Delta(\Delta G^\circ)_{TAG} - \Delta(\Delta G^\circ)_T$ ] with very few exceptions, are negative, i.e., the interaction between the free aglycone basket (without the sugar moieties) and analyte improves chiral recognition. By comparing the [ $\Delta(\Delta G^\circ)_{TAG} - \Delta(\Delta G^\circ)_T$ ] values for analytes **1-6**, it is interesting to note that in the case of molecules with a larger size, interactions between selector and analyte are favored. It should be noted that [ $\Delta(\Delta G^\circ)_{TAG} - \Delta(\Delta G^\circ)_T$ ] values can vary with the amount of mobile phase additives.

### 3.5. van Deemter analysis

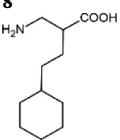
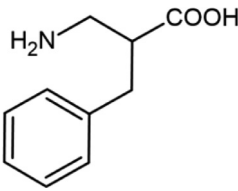
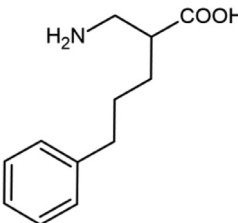
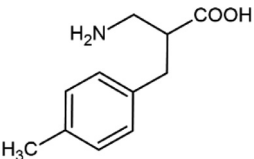
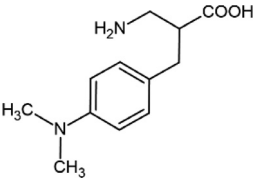
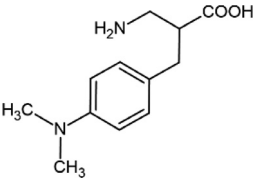
Organic components of eluents (MeOH and MeCN) used in this study in combination with water yield mobile phases with considerable viscosity, while combination of MeOH and MeCN result in low-viscosity eluent allowing higher flow rates without high backpressures. According to Darcy's law, backpressure relates to mobile phase viscosity and linear velocity [21,36]. For the investigation of van Deemter plots, mobile phases possessing low and moderate viscosity [mobile phase **b**, aq. TEAA/MeOH (30/70 v/v) and **c**, MeCN/MeOH (30/70 v/v), respectively] both containing 2.5 mM TEA and 5.0 mM AcOH] were selected, and plots were constructed on all four studied columns for analytes containing an aliphatic (**6**) or

**Table 1**  
Selected chromatographic data for the separation of  $\beta^2$ -amino acids

Analyte	Column	Mobile phase	$k_1$	$\alpha$	$R_S$
<b>aliphatic <math>\beta^2</math>-amino acids</b>					
<b>1</b>	T-3.0	H <sub>2</sub> O/MeOH (30/70 v/v)	0.40	1.30	1.01
	T-3.0	H <sub>2</sub> O/MeOH (10/90 v/v)	0.20	1.46	0.90
	TAG-3	H <sub>2</sub> O/MeOH (30/70 v/v)	0.70	1.30	1.05
	TAG-3	H <sub>2</sub> O/MeOH (10/90 v/v)	1.82	1.22	0.72
	TAG-3.0	aq.TEAA/MeOH (10/90 v/v)	1.75	1.24	0.74
	T-3.0	aq.TEAA/MeOH (30/70 v/v)	0.53	1.35	1.32
<b>2</b>					
	TAG-3.0	H <sub>2</sub> O/MeOH (30/70 v/v)	0.50	1.54	1.35
	T-3.0	H <sub>2</sub> O/MeOH (30/70 v/v)	0.34	1.75	2.48
	T-2.1	H <sub>2</sub> O/MeOH (30/70 v/v)	0.86	1.30	1.58
<b>3</b>					
	T-3.0	H <sub>2</sub> O/MeOH (30/70 v/v)	0.47	1.80	2.66
	TAG-3.0	MeCN/MeOH (30/70 v/v)	1.49	1.63	1.71
	TAG-2.1	MeCN/MeOH (30/70 v/v)	1.04	1.72	1.53
	T-3.0	H <sub>2</sub> O/MeOH (30/70 v/v)	0.33	1.76	2.07
<b>4</b>					
	TAG-3.0	MeCN/MeOH (30/70 v/v)	1.37	1.60	1.70
	TAG-2.1	MeCN/MeOH (30/70 v/v)	0.97	1.66	1.40
	T-3.0	H <sub>2</sub> O/MeOH (30/70 v/v)	0.30	1.85	1.71
	TAG-3.0	H <sub>2</sub> O/MeOH (30/70 v/v)	0.45	1.90	1.35
<b>5</b>					
	TAG-3.0	MeCN/MeOH (30/70 v/v)	1.02	1.73	1.37
	TAG-3.0	MeCN/MeOH (10/90 v/v)	1.09	1.51	1.58
	T-3.0	H <sub>2</sub> O/MeOH (30/70 v/v)	0.28	2.03	2.50
	T-3.0	MeCN/MeOH (10/90 v/v)	1.45	1.45	0.83
<b>6</b>					
	T-2.1	H <sub>2</sub> O/MeOH (30/70 v/v)	0.85	1.46	1.64
	TAG-3.0	H <sub>2</sub> O/MeOH (30/70 v/v)	0.95	2.06	2.39
	TAG-3.0	aq.TEAA/MeOH (30/70 v/v)	0.22	1.74	1.30
	TAG-3.0	aq.TEAA/MeOH (10/90 v/v)	0.73	2.24	2.88
	TAG-3.0	MeCN/MeOH (30/70 v/v)	1.15	1.82	2.02
	TAG-2.1	H <sub>2</sub> O/MeOH (30/70 v/v)	0.77	1.48	1.72
	TAG-2.1	MeCN/MeOH (30/70 v/v)	0.69	1.90	1.89
	T-3.0	H <sub>2</sub> O/MeOH (30/70 v/v)	0.27	1.81	1.97
<b>7</b>					
	TAG-3.0	H <sub>2</sub> O/MeOH (30/70 v/v)	0.66	1.64	1.80
	TAG-3.0	aq.TEAA/MeOH (20/80 v/v)	0.28	1.62	1.14
	TAG-3.0	aq.TEAA/MeOH (10/90 v/v)	0.79	1.80	2.08
	TAG-3.0	MeCN/MeOH (30/70 v/v)	1.08	1.60	1.77

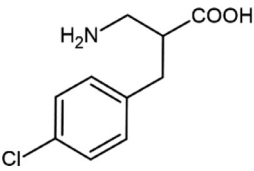
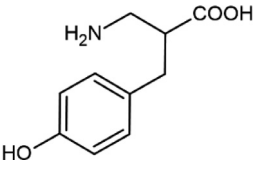
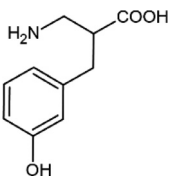
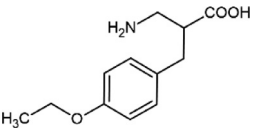
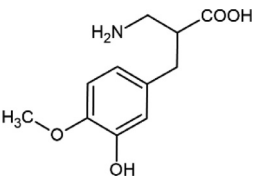
(continued on next page)

Table 1 (continued)

Analyte	Column	Mobile phase	$k_f$	$\alpha$	$R_S$
<b>8</b> 	T-3.0	H <sub>2</sub> O/MeOH (30/70 v/v)	1.10	1.59	2.05
	T-3.0	aq.TEAA/MeOH (10/90 v/v)	0.79	1.61	1.67
	TAG-3.0	MeCN/MeOH (30/70 v/v)	1.55	1.56	1.75
<b>aromatic <math>\beta^2</math>-amino acids</b> <b>9</b> 	T-3.0	H <sub>2</sub> O/MeOH (30/70 v/v)	0.82	1.36	1.75
	T-3.0	aq.TEAA/MeOH (30/70 v/v)	0.62	1.48	1.99
	T-2.1	H <sub>2</sub> O/MeOH (30/70 v/v)	1.73	1.23	1.94
	T-2.1	aq.TEAA/MeOH (30/70 v/v)	0.69	1.53	1.73
<b>10</b> 	T-2.1	MeCN/MeOH (30/70 v/v)	2.43	1.39	1.68
	TAG-3.0	H <sub>2</sub> O/MeOH (30/70 v/v)	1.00	1.49	1.82
	TAG-3.0	aq.TEAA/MeOH (30/70 v/v)	0.91	1.49	1.94
	TAG-2.1	H <sub>2</sub> O/MeOH (30/70 v/v)	1.09	1.34	1.59
	TAG-2.1	aq.TEAA/MeOH (30/70 v/v)	0.72	1.60	1.72
	TAG-2.1	MeCN/MeOH (30/70 v/v)	1.67	1.48	1.68
	T-3.0	H <sub>2</sub> O/MeOH (30/70 v/v)	0.97	1.50	1.74
	T-3.0	aq.TEAA/MeOH (30/70 v/v)	0.62	1.70	2.77
	T-3.0	MeCN/MeOH (30/70 v/v)	1.88	1.43	1.76
	T-2.1	H <sub>2</sub> O/MeOH (30/70 v/v)	1.74	1.21	1.87
	T-2.1	aq.TEAA/MeOH (30/70 v/v)	0.72	1.72	2.40
	T-2.1	MeCN/MeOH (30/70 v/v)	2.07	1.52	2.08
	TAG-3.0	H <sub>2</sub> O/MeOH (30/70 v/v)	1.19	1.73	2.83
	TAG-3.0	aq.TEAA/MeOH (30/70 v/v)	1.10	1.74	3.02
	TAG-3.0	MeCN/MeOH (30/70 v/v)	2.05	1.71	2.06
	TAG-2.1	H <sub>2</sub> O/MeOH (30/70 v/v)	1.24	1.46	2.31
TAG-2.1	aq.TEAA/MeOH (30/70 v/v)	0.89	1.75	2.50	
TAG-2.1	MeCN/MeOH (30/70 v/v)	1.45	1.80	2.54	
<b>11</b> 	T-3.0	aq.TEAA/MeOH (30/70 v/v)	0.64	1.39	1.70
	T-2.1	H <sub>2</sub> O/MeOH (30/70 v/v)	1.87	1.17	1.58
	T-2.1	aq.TEAA/MeOH (30/70 v/v)	0.72	1.46	1.59
<b>12</b> 	T-2.1	MeCN/MeOH (30/70 v/v)	2.30	1.33	1.46
	TAG-3.0	aq.TEAA/MeOH (30/70 v/v)	1.12	1.43	1.68
	TAG-3.0	MeCN/MeOH (30/70 v/v)	1.02	1.41	1.78
	TAG-2.1	H <sub>2</sub> O/MeOH (30/70 v/v)	1.39	1.39	2.02
	TAG-2.1	aq.TEAA/MeOH (30/70 v/v)	0.81	1.51	1.64
	TAG-2.1	MeCN/MeOH (30/70 v/v)	1.58	1.45	1.64
	T-3.0	aq.TEAA/MeOH (30/70 v/v)	1.57	1.17	1.27
	T-3.0	aq.TEAA/MeOH (10/90 v/v)	1.88	1.44	1.97
T-2.1	MeCN/MeOH (30/70 v/v)	2.95	1.32	1.37	
<b>12</b> 	T-2.1	MeCN/MeOH (10/90 v/v)	2.35	1.27	1.19
	TAG-3.0	MeCN/MeOH (30/70 v/v)	2.62	1.33	1.06
	TAG-3.0	MeCN/MeOH (10/90 v/v)	3.08	1.39	1.15
	TAG-2.1	MeCN/MeOH (20/80 v/v)	1.81	1.43	1.53

(continued on next page)

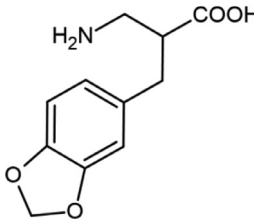
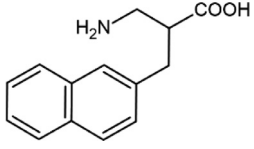
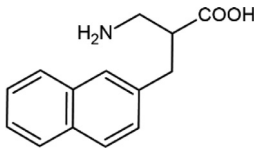
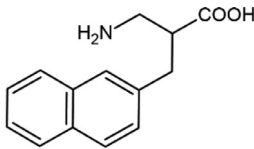
Table 1 (continued)

Analyte	Column	Mobile phase	$k'_1$	$\alpha$	$R_S$
	T-3.0	aq.TEAA/MeOH (30/70 v/v)	0.73	1.18	1.32
	T-3.0	aq.TEAA/MeOH (10/90 v/v)	1.30	1.32	1.56
	T-2.1	aq.TEAA/MeOH (30/70 v/v)	0.78	1.30	1.32
	T-2.1	aq.TEAA/MeOH (10/90 v/v)	1.62	1.40	1.91
	TAG-3.0	aq.TEAA/MeOH (30/70 v/v)	1.33	1.26	1.22
	TAG-3.0	aq.TEAA/MeOH (10/90 v/v)	2.08	1.28	1.07
	TAG-2.1	H <sub>2</sub> O/MeOH (30/70 v/v)	1.60	1.28	1.47
	TAG-2.1	aq.TEAA/MeOH (30/70 v/v)	1.04	1.35	1.21
	TAG-2.1	aq.TEAA/MeOH (10/90 v/v)	1.49	1.38	1.46
		T-3.0	aq.TEAA/MeOH (30/70 v/v)	0.67	1.46
T-2.1		H <sub>2</sub> O/MeOH (30/70 v/v)	1.71	1.16	1.49
T-2.1		aq.TEAA/MeOH (30/70 v/v)	0.73	1.51	1.74
T-2.1		MeCN/MeOH (30/70 v/v)	2.47	1.37	1.59
TAG-3.0		H <sub>2</sub> O/MeOH (30/70 v/v)	0.83	1.48	1.89
TAG-3.0		aq.TEAA/MeOH (30/70 v/v)	0.95	1.96	3.32
TAG-3.0		MeCN/MeOH (30/70 v/v)	2.63	1.43	1.38
TAG-2.1		H <sub>2</sub> O/MeOH (30/70 v/v)	1.11	1.39	2.09
TAG-2.1		aq.TEAA/MeOH (30/70 v/v)	0.74	2.13	2.78
TAG-2.1		MeCN/MeOH (30/70 v/v)	1.88	1.53	1.91
	T-3.0	H <sub>2</sub> O/MeOH (30/70 v/v)	0.86	1.40	1.57
	T-3.0	aq.TEAA/MeOH (30/70 v/v)	0.59	1.50	3.10
	T-3.0	MeCN/MeOH (30/70 v/v)	2.31	1.36	1.38
	TAG-3.0	H <sub>2</sub> O/MeOH (30/70 v/v)	0.82	2.10	2.58
	T-3.0	aq.TEAA/MeOH (30/70 v/v)	0.68	1.34	1.51
	T-2.1	H <sub>2</sub> O/MeOH (30/70 v/v)	1.92	1.16	1.50
	T-2.1	aq.TEAA/MeOH (30/70 v/v)	0.76	1.41	1.48
	TAG-3.0	H <sub>2</sub> O/MeOH (30/70 v/v)	1.12	1.37	1.48
	TAG-3.0	aq.TEAA/MeOH (30/70 v/v)	1.07	1.36	1.63
	TAG-2.1	H <sub>2</sub> O/MeOH (30/70 v/v)	1.47	1.34	1.90
	TAG-2.1	aq.TEAA/MeOH (30/70 v/v)	0.85	1.44	1.53
	TAG-2.1	MeCN/MeOH (30/70 v/v)	1.63	1.41	1.51
	T-3.0	aq.TEAA/MeOH (30/70 v/v)	0.67	1.45	1.82
	T-2.1	H <sub>2</sub> O/MeOH (30/70 v/v)	1.86	1.18	1.57
	T-2.1	aq.TEAA/MeOH (30/70 v/v)	0.73	1.50	1.74
	TAG-3.0	H <sub>2</sub> O/MeOH (30/70 v/v)	0.92	2.00	2.91
	TAG-3.0	aq.TEAA/MeOH (30/70 v/v)	0.93	1.93	3.16
	TAG-3.0	MeCN/MeOH (30/70 v/v)	2.91	1.70	2.14
TAG-2.1	H <sub>2</sub> O/MeOH (30/70 v/v)	1.26	1.74	3.00	
TAG-2.1	aq.TEAA/MeOH (30/70 v/v)	0.74	2.12	2.78	
TAG-2.1	MeCN/MeOH (30/70 v/v)	2.13	1.83	2.64	

(continued on next page)



Table 1 (continued)

Analyte	Column	Mobile phase	$k_1$	$\alpha$	$R_S$	
<b>18</b> 	T-3.0	H <sub>2</sub> O/MeOH (30/70 v/v)	1.19	1.35	1.58	
	T-3.0	aq.TEAA/MeOH (30/70 v/v)	0.74	1.47	2.09	
	T-3.0	MeCN/MeOH (30/70 v/v)	2.37	1.32	1.48	
	T-2.1	H <sub>2</sub> O/MeOH (30/70 v/v)	2.02	1.22	1.91	
	T-2.1	aq.TEAA/MeOH (30/70 v/v)	0.84	1.52	1.94	
	T-2.1	MeCN/MeOH (30/70 v/v)	2.71	1.40	1.74	
	TAG-3.0	H <sub>2</sub> O/MeOH (30/70 v/v)	1.05	1.73	2.72	
	TAG-3.0	aq.TEAA/MeOH (30/70 v/v)	1.07	1.66	2.75	
	TAG-3.0	MeCN/MeOH (30/70 v/v)	2.50	1.55	1.68	
	TAG-2.1	H <sub>2</sub> O/MeOH (30/70 v/v)	1.44	1.56	2.88	
	TAG-2.1	aq.TEAA/MeOH (30/70 v/v)	0.84	1.77	2.46	
	TAG-2.1	MeCN/MeOH (30/70 v/v)	1.76	1.66	2.27	
	<b>19</b> 	T-3.0	H <sub>2</sub> O/MeOH (30/70 v/v)	1.17	1.45	1.98
		T-3.0	aq.TEAA/MeOH (30/70 v/v)	0.75	1.64	2.71
		T-3.0	MeCN/MeOH (30/70 v/v)	2.27	1.36	1.55
<b>19</b> 	T-2.1	H <sub>2</sub> O/MeOH (30/70 v/v)	1.97	1.31	2.37	
	T-2.1	aq.TEAA/MeOH (30/70 v/v)	0.88	1.70	2.57	
	T-2.1	MeCN/MeOH (30/70 v/v)	2.96	1.45	1.94	
	TAG-3.0	H <sub>2</sub> O/MeOH (30/70 v/v)	1.53	1.75	2.77	
<b>19</b> 	TAG-3.0	aq.TEAA/MeOH (30/70 v/v)	1.62	1.73	2.97	
	TAG-3.0	MeCN/MeOH (30/70 v/v)	2.95	1.53	1.50	
	TAG-2.1	H <sub>2</sub> O/MeOH (30/70 v/v)	1.60	1.67	3.22	
	TAG-2.1	aq.TEAA/MeOH (30/70 v/v)	1.04	1.86	2.83	
	TAG-2.1	MeCN/MeOH (30/70 v/v)	2.12	1.69	2.30	

Chromatographic conditions: column, **T-3.0**, **T-2.1**, **TAG-3.0** and **TAG-2.1**; mobile phase, H<sub>2</sub>O/MeOH (30/70 v/v), aq.TEAA/MeOH (30/70 v/v) and MeCN/MeOH (30/70 v/v), the latter two contain 2.5 mM TEA and 5.0 mM AcOH; flow rate, 0.3 ml min<sup>-1</sup>; detection, 210–258 nm; temperature, 20 °C

aromatic (**9**) side chain. van Deemter plots are shown in Figure 8 A (for analyte **6**) and Fig. S5 A (for analyte **9**) in polar-ionic mode. In the polar-ionic mode, the curves for the first eluting enantiomer show characteristic minima for analyte **6** on **T-3.0**, **T-2.1**, and **TAG-3.0** columns, and a slight minima on **TAG-2.1** at ~1.5 mm sec<sup>-1</sup> (Fig. 8 A). It should be noted that 2.1 mm i.d. columns are usually less efficient than 3.0 mm ones due to wall effects (Fig. 8 A). The H minima on **T-3.0** and **TAG-3.0** were registered at 0.24 mm sec<sup>-1</sup>, while on **T-2.1** at 0.48 mm sec<sup>-1</sup> linear velocity, which corresponds to a flow rate of 0.1 ml min<sup>-1</sup>. The van Deemter curves for teicoplanin-based columns run below the plots of the teicoplanin aglycone. Fig. S5 A depicts van Deemter plots for analyte **9** under the same conditions. The shape of the curve for columns with 3.0 mm i.d. are similar to plots obtained for analyte **6** (minima are in the range 0.24–0.48 mm sec<sup>-1</sup>, i.e., 0.1–0.2 ml min<sup>-1</sup>), while plots obtained on columns with 2.1 mm i.d. exhibited slight minima at lower flow rates (0.05–0.1 ml min<sup>-1</sup>). Interestingly, the H-u plot for the teicoplanin aglycone column with 2.1 mm i.d. (**TAG-2.1**) runs below the same type of column with a larger i.d. (**TAG-3.0**). Figures 8B and S5B depict van Deemter plots for analytes **6** and **9** applying mobile phase **b**, aq.TEAA/MeOH (30/70 v/v) containing 2.5 mM TEA and 5.0 mM AcOH on teicoplanin- and te-

icoplanin aglycone-based columns possessing different internal diameters. The van Deemter curves at high flow rates (where the C-term dominates) on **T-3.0** columns exhibited a slight increase in plate height, while on **T-2.1** columns a decrease in plate height (slightly negative slope) was registered for both analytes at high flow rates. It is described several times that at high backpressures, two types of temperature gradients – axial and radial – exist together as the result of significant frictional heating [16,37–39]. Axial temperature differences ranging from 11 to 16 °C can readily be generated when pressure above 300 bar is applied [16,37]. In some cases, longitudinal frictional heating was found to increase the chiral resolution when small particles and high flow rates are used [16,21]. In Fig. 8 C, van Deemter plots for the first and second eluting enantiomer of analyte **6** on **TAG-3** and analyte **9** on the **T-2.1** column are depicted. It is interesting to note that identical kinetic plot shapes were recorded for both enantiomers with the curve for the second enantiomer shifted upwards. The similar shapes indicate that both enantiomers have similar adsorption/desorption kinetics (the same results were obtained under other conditions too; data not shown). In summary, comparing results obtained for van Deemter analyses and screening experiments of 19 β<sup>2</sup>-amino acids (registered at a flow rate of 0.3 ml min<sup>-1</sup>), the following conclu-

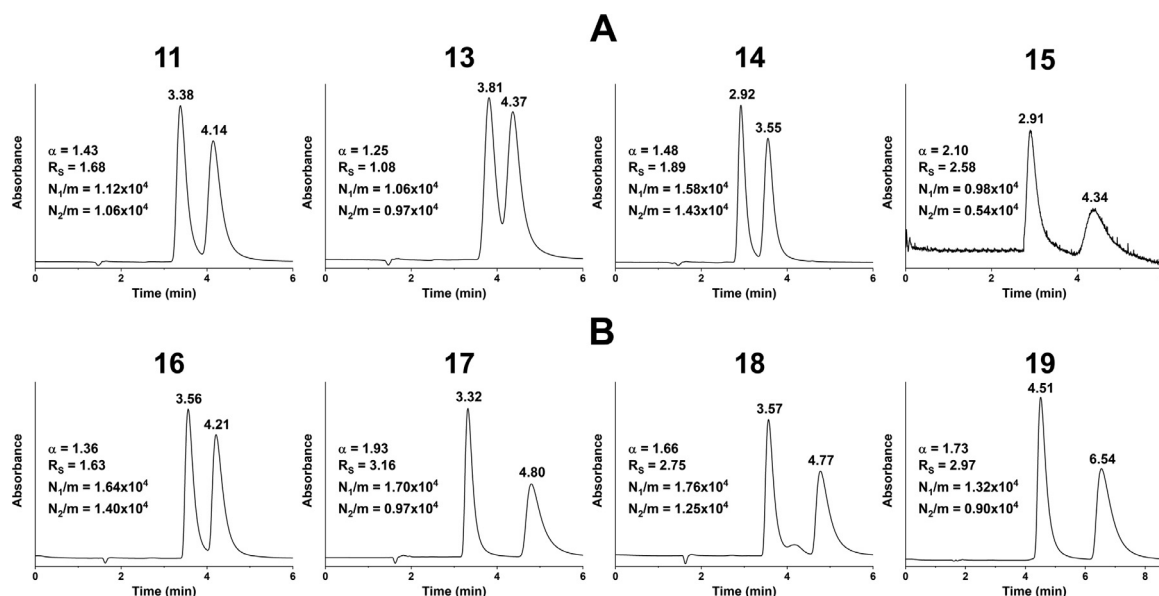


**Figure 5.** Effect of nature of substituents and chemical structure of analytes on chromatographic performance for analytes **11** and **13-19**. Chromatographic conditions, column, TAG-3.0; mobile phase, **A**, H<sub>2</sub>O/MeOH (30/70 v/v), **B**, aq.TEAA/MeOH (30/70 v/v), concentration of TEA and AcOH in mobile phase 2.5 and 5.0 mM, respectively and the actual pH of the mobile phase, pH<sub>a</sub> 5.5; flow rate, 0.3 ml min<sup>-1</sup>; detection, 258 nm; temperature, 20 °C

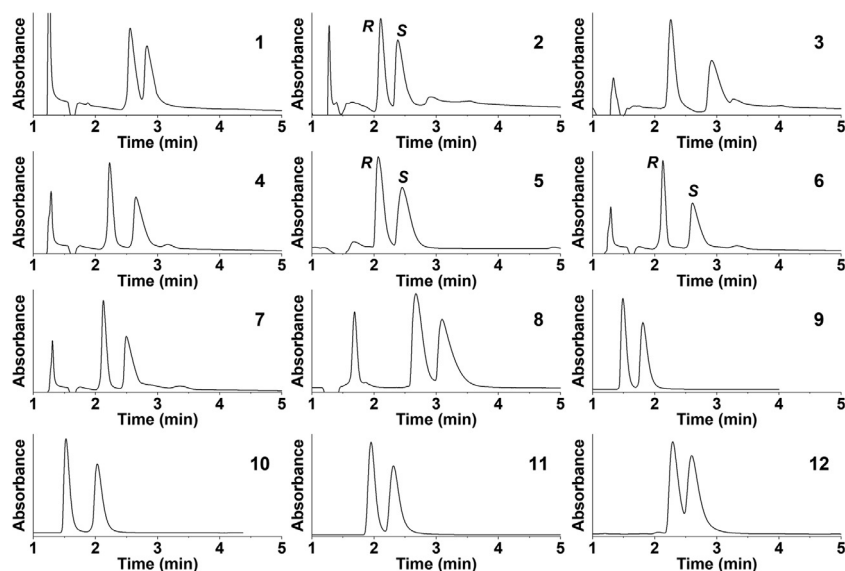


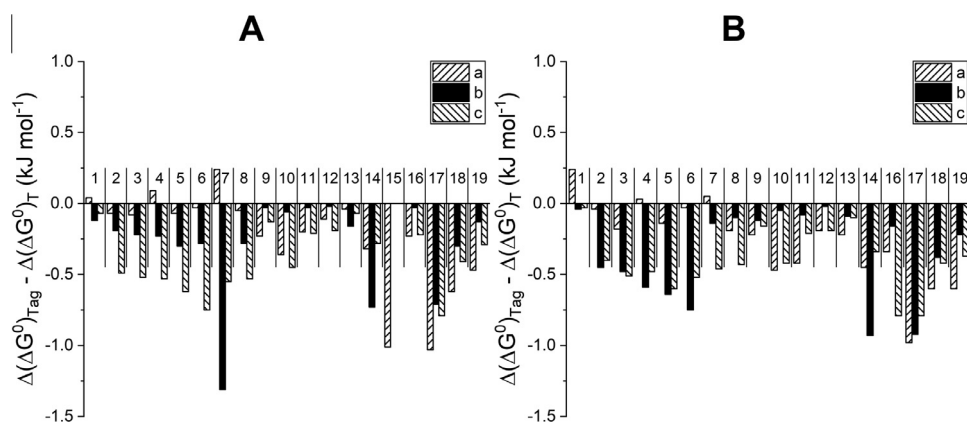
**Figure 6.** Selected chromatograms for analytes **1-10** and **12**. Chromatographic conditions, columns, for analytes **1, 4, 6, 7, and 8** T-3.0, for **2, 3** and **5** TAG-3.0, for **9** and **10** T-2.1 and for **11** and **12** TAG-2.1; mobile phase, for analytes **1-7** and **11**, H<sub>2</sub>O/MeOH (30/70 v/v), for **8-10** and **12** aq.TEAA/MeOH (30/70 v/v), concentration of TEA and AcOH in mobile phase 2.5 and 5.0 mM, respectively and the actual pH of the mobile phase, pH<sub>a</sub> 5.5; flow rate, 0.3 ml min<sup>-1</sup>; detection, 258 nm; temperature, 20 °C;



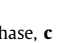
sions can be drawn: (i) higher plate numbers were obtained on teicoplanin-based than on teicoplanin aglycone-based CSP (**T-3.0** vs. **TAG-3.0** and **T-2.1** vs. **TAG-2.1**), (ii) in general, for SPPs of 2.7  $\mu$ m, the narrow bore columns (2.1 mm i.d.) show decreased efficiency compared to their counterparts with 3.0 mm i.d. Note, that the latter columns were expected to outperform the columns of 2.1 mm i.d., and this expectation was met under all the studied conditions. It must be emphasized, however, that column performance, in the practice, depends on both the nature of analytes and the mobile phase composition. H values for analytes possessing an alkyl side chain (**1-8**) were always smaller on columns of 3.0 mm i.d., while for analytes possessing an aromatic side chain (**9-19**), columns of 2.1 mm i.d. showed better performance (Table S1-S4 and Fig. S5 A). However, in the RP mode for analytes **9-19**, columns of 3.0 mm i.d. always outperformed the columns of 2.1 mm i.d. columns (Table S1-S4).

### 3.6. Temperature dependence and thermodynamic parameters

Studying the effects of temperature on retention and enantioselectivity in chiral separations is an often applied methodology to gather information on enantiomer recognition [40-43]. Theoretically, retention observed on chiral CSPs consists of chiral and nonchiral components [44-48], however, in this study, these two components are not differentiated. Keeping in mind the limitations of the approach, used herein the difference in the change in standard enthalpy  $\Delta(\Delta H^\circ)$  and entropy  $\Delta(\Delta S^\circ)$  for the enantiomer pairs were calculated using the relationship between  $\ln \alpha$  (natural logarithm of the apparent selectivity factor) and  $T^{-1}$  (reciprocal of absolute temperature) as described by the van't Hoff equation:

$$\ln \alpha = -\frac{\Delta(\Delta H^\circ)}{RT} + \frac{\Delta(\Delta S^\circ)}{R} \quad (2)$$



**Figure 7.** Enantioselectivity free energy differences  $\Delta(\Delta G^\circ)_{TAG} - \Delta(\Delta G^\circ)_T$  between aglycone and native teicoplanin selector Chromatographic condition, column, **A**, TAG-3.0 vs. T-3.0 and **B**, TAG-2.1 vs. T-2.1; mobile phase, **a**, H<sub>2</sub>O/MeOH 30/70 v/v, **b**, *aq*.TEAA/MeOH (30/70 v/v), concentration of TEA and AcOH in the mobile phase 2.5 and 5.0 mM, respectively, and the actual pH of the mobile phase, pH<sub>a</sub> 5.5, **c**, MeCN/MeOH (30/70 v/v), concentration of TEA and AcOH in the mobile phase 2.5 and 5.0 mM, respectively; flow rate, 0.3 ml min<sup>-1</sup>; detection, 210–258 nm; temperature, 20 °C; symbols, mobile phase, **a**, , mobile phase, **b**,  and mobile phase, **c**, 

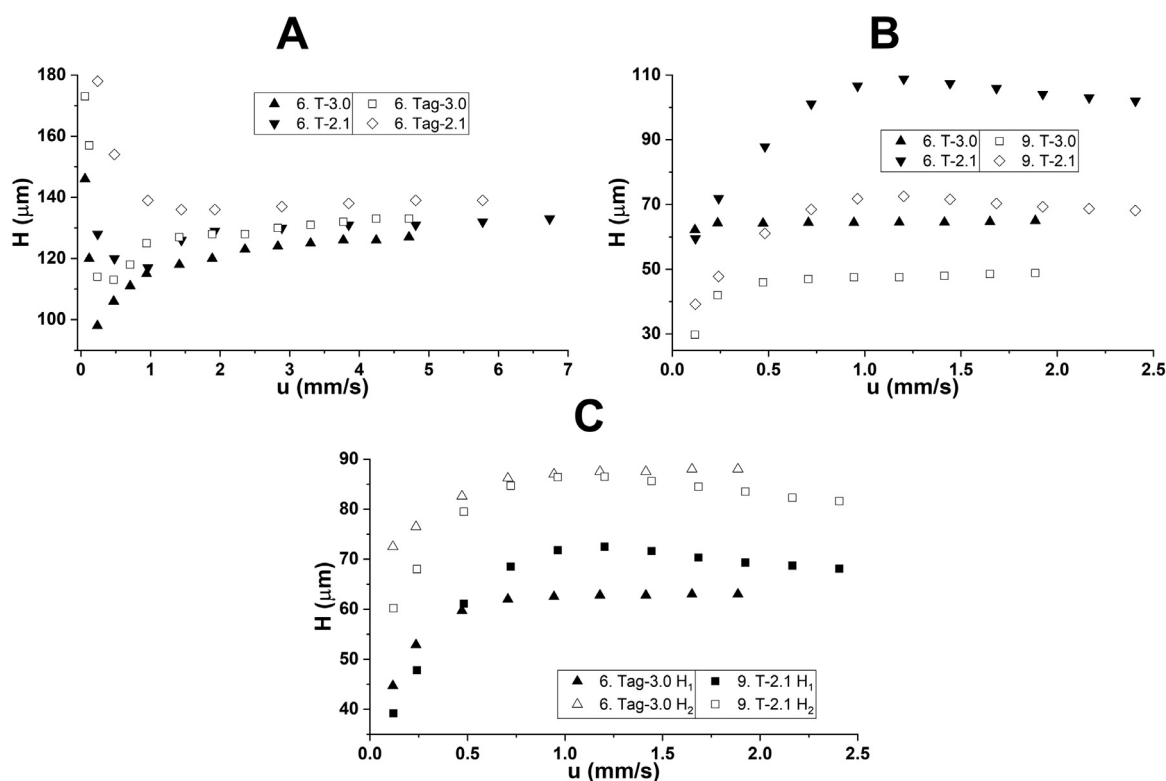


**Figure 8.** Plots of plate heights versus superficial velocities for analytes **6** and **9** on macrocyclic glycopeptide-based columns Chromatographic conditions: columns, **A**, T-3.0, T-2.1, TAG-3.0 and TAG-2.1, **B**, T-3.0, T-2.1 and **C**, TAG-3.0 and T-2.1; mobile phase, **A**, MeCN/MeOH (30/70 v/v), concentration of TEA and AcOH in the mobile phase 2.5 and 5.0 mM, respectively, **B** and **C**, *aq*.TEAA/MeOH (30/70 v/v), concentration of TEA and AcOH in the mobile phase 2.5 and 5.0 mM, respectively, and the actual pH<sub>a</sub> of the mobile phase, pH<sub>a</sub> 5.5; detection, 210–258 nm; temperature, 20 °C; symbols, **A**, analyte **6**, ▲ T-3.0, ▼ T-2.1, □ TAG-3.0, ◇ TAG-2.1; **B**, analyte **6**, ▲ T-3.0, ▼ T-2.1, analyte **9**, □ T-3.0, ◇ T-2.1; **C**, analyte **6**, ▲ TAG-3.0 (first enantiomer), △ TAG-3.0 (second enantiomer), analyte **9**, ■ T-2.1 (first enantiomer), □ T-2.1 (second enantiomer)

where  $R$  is the universal gas constant. As discussed earlier, under UHPLC conditions operating with inlet pressures above 300 bars, the generated axial temperature differences can lead to a marked difference between real operational and set conditions [16,21,37]. To avoid the temperature differences caused by high backpressure, the nature of applied mobile phases and flow rates were carefully selected for this study. For example, CSPs with 2.1 mm i.d. were applied only in polar-ionic mode.

Dependence of the chromatographic parameters on temperature was studied on the four columns for analyte **8** possessing an aliphatic side chain, and for analyte **9** bearing an aromatic

side chain in the temperature range 5–50 °C. Experimental data with mobile phases of *aq*.TEAA/MeOH (30/70 v/v) and MeCN/MeOH (30/70 v/v) both containing 20 mM TEAA are presented in Table S5. As most frequently observed, both  $k$  and  $\alpha$  decreased with increasing temperature in all cases. Resolution usually decreases with increasing temperature, while in a few cases,  $R_S$  exhibited a maximum curve with the change of temperature (Table S5). Lower  $R_S$  values at low and high temperatures can be attributed to the lower kinetic and higher thermodynamic effect (decreased  $\alpha$  values), respectively.

**Table 2**

Thermodynamic parameters,  $\Delta(\Delta H^\circ)$ ,  $\Delta(\Delta S^\circ)$ ,  $T_x\Delta(\Delta S^\circ)$ ,  $\Delta(\Delta G^\circ)$ , correlation coefficients ( $R^2$ ),  $T_{iso}$  and  $Q$  values of  $\beta^2$ -amino acids in different separation modalities on **TeicoShell** and **TagShell** columns with 3.0 and 2.1 i.d., respectively

Compound	Mobile phase	$-\Delta(\Delta H^\circ)$ (kJ/mol)	$-\Delta(\Delta S^\circ)$ (J/(mol·K))	Correlation coefficients ( $R^2$ )	$-T_x\Delta(\Delta S^\circ)_{298K}$ (kJ/mol)	$-\Delta(\Delta G^\circ)_{298K}$ (kJ/mol)	$T_{iso}$ (°C)	$Q$
<b>TeicoShell (3.0 mm I.D.)</b>								
<b>8</b>	<b>b</b>	3.55	7.59	0.9960	2.26	1.28	194	1.57
	<b>c</b>	1.43	2.72	0.9790	0.81	0.62	255	1.77
<b>9</b>	<b>b</b>	2.05	3.57	0.9882	1.06	0.99	302	1.93
	<b>c</b>	1.30	2.31	0.9976	0.69	0.61	289	1.89
<b>TeicoShell (2.1 mm I.D.)</b>								
<b>8</b>	<b>c</b>	1.96	4.32	0.9936	1.29	0.68	181	1.52
<b>9</b>	<b>c</b>	1.99	3.99	0.9994	1.19	0.80	226	1.67
<b>TagShell (3.0 mm I.D.)</b>								
<b>8</b>	<b>b</b>	2.04	4.42	0.9912	1.32	0.73	189	1.55
	<b>c</b>	2.56	5.14	0.9949	1.53	1.02	225	1.67
<b>9</b>	<b>b</b>	2.06	4.24	0.9810	1.26	0.79	212	1.63
	<b>c</b>	2.11	4.78	0.9980	1.42	0.68	168	1.48
<b>TagShell (2.1 mm I.D.)</b>								
<b>8</b>	<b>c</b>	2.02	3.34	0.9950	0.99	1.02	332	2.03
<b>9</b>	<b>c</b>	2.28	4.91	0.9989	1.46	0.81	191	1.56

Chromatographic conditions: columns, **TeicoShell** and **TagShell** with **3.0** and **2.1** i.d., respectively; mobile phase, **b**, *aq*.TEAA/MeOH/ (30/70 v/v), total concentration of TEAA in the mobile phase 20 mM, actual pH of mobile phase,  $pH_a = 5.0$ , **c**, MeCN/MeOH/ (30/70 v/v) containing 20 mM TEAA; detection, 215–256 nm; flow rates, 0.3 ml min<sup>-1</sup>;  $T_{iso}$ , temperature where the enantioselectivity cancels;  $Q = \Delta(\Delta H^\circ) / T \times \Delta(\Delta S^\circ)_{298K}$

The calculated  $-\Delta(\Delta H^\circ)$  and  $-\Delta(\Delta S^\circ)$  values are presented in Table 2. The  $\Delta(\Delta H^\circ)$  values ranged from  $-1.30$  to  $-3.55$  kJ mol<sup>-1</sup>. These negative values indicate that the adsorption/desorption kinetics are enthalpically favored.  $\Delta(\Delta S^\circ)$  values ranged from  $-2.31$  to  $-7.59$  J mol<sup>-1</sup> K<sup>-1</sup>. It is important to note that  $\Delta(\Delta S^\circ)$  values are depended on (i) the difference in the number of degrees of freedom between the solutes bound on the CSP, and (ii) the number of solvent molecules leaving the solvated CSP and the analyte, when the analyte is associated with the CSP. The trends in the change in  $\Delta(\Delta S^\circ)$  and  $\Delta(\Delta H^\circ)$  were similar, that is, a more negative  $\Delta(\Delta H^\circ)$  was accompanied by a more negative  $\Delta(\Delta S^\circ)$ .

Under the applied conditions more negative  $\Delta(\Delta G^\circ)$  values (calculated at 298 K) were obtained on TagShell CSPs, in most cases, indicating that the differential binding to the aglycone-based selector was more favorable. For the representation of the relative contribution to the free energy of adsorption we calculated the enthalpy/entropy ratio, as  $Q = \Delta(\Delta H^\circ)/[298 \times \Delta(\Delta S^\circ)]$ . As indicated in Table 2, the enantioselective discrimination was enthalpically driven in all cases.

#### 4. Conclusions

It was generally observed that an increase in the methanol content in the RP mode resulted in a slight increase in retention and moderate enhancement in selectivity and resolution. In the polar-ionic mode, retention considerably decreased, while selectivity and resolution moderately increased with increasing methanol content. The change of actual  $pH_a$  under RP conditions showed, that  $pH_a$  values higher than 5.0 were advantageous regarding retention, selectivity, and resolution. In the application of different organic acids and salts, the best chromatographic performances were observed with the TEAA additive.

Macrocyclic glycopeptide CSPs are expected to act as weak ion-exchangers and this concept was supported by the validated displacement model. Investigation of the effect of analyte and selector structures revealed that (i) there is a strong relationship between separation performance (retention and selectivity) and the size of the aliphatic side chain (Meyer's size descriptor), (ii) the nature of substituents on analytes with an aromatic ring (endowing  $\pi$ -acidic- or  $\pi$ -basic character for the molecule) affects separation performance slightly, while the position of a hydroxyl moiety has a considerable effect, and (iii) separation is thermodynamically favored in the case of selectors without sugar units (aglycone-based CSPs).

Analyses of van Deemter plots in the polar-ionic mode confirmed a typical shape with a plate height of minima, while no characteristic minima were registered when RP eluents were applied. Columns with 3.0 mm i.d. exhibited a slight increase in plate height, while a decrease in plate height was registered for the columns with 2.1 mm i.d. at high flow rates (axial temperature effect). In addition, in all three mobile phase systems, lower plate heights were obtained: (i) concerning native teicoplanin (**T**) vs. teicoplanin aglycone (**TAG**) for all analytes and (ii) concerning columns with 3.0 mm i.d. vs. columns with 2.1 mm i.d. for  $\beta^2$ -amino acids possessing aliphatic side chains. For analytes with aromatic side chains, an opposite correlation was observed. Evaluation of the kinetic curves, in most cases, supports that the separation of two enantiomers takes place with the same adsorption/desorption kinetics, i.e., the shape and slope of van Deemter plots were similar. Let us note here, that the determined plate heights were higher than expected, although data were not corrected with the extra-column volume of the instrument. Reduction of the extra-column effects (e.g., by altering the tubing of the UHPLC) would probably result in lower plate heights. The flat C-term curves observed in many cases demonstrate the possibility for high-speed enantioseparations without significant loss in efficiency, thus the speed gain and the significant reduction in solvent consumption offered by the columns based on 2.7  $\mu$ m SP particles compared to a traditional (5  $\mu$ m FP particle-based) column are worth to utilize.

Thermodynamic parameters obtained by a temperature-dependence study revealed that enantioseparations were enthalpically driven and selectivity decreased with enhanced temperature under all studied conditions.

Elution sequences for analytes **2**, **5**, and **6** were determined to show an  $R < S$  relationship.

#### Declaration of Competing Interest

The authors declare no conflict of interest.

#### Acknowledgments

This work was supported by the National Research Development and Innovation Office, project grant GINOP-2.3.2-15-2016-00034, the EU-funded Hungarian grant EFOP-3.6.1-16-2016-00008, and the Ministry of Human Capacities, Hungary grant TKP-2020.

## Credit Author Statement

**Dániel Tanács:** Investigation, Writing – Original Draft, Visualization; **Róbert Berkecz:** Conceptualization, Writing– Original Draft, Review & Editing; **Aleksandra Misicka, Dagmara Tymecka:** Resources, Writing – Original Draft; **Ferenc Fülöp:** Writing– Review & Editing, **Daniel Armstrong:** Conceptualization, Writing– Original Draft, Review & Editing; **Antal Péter:** Conceptualization, Writing–Review & Editing; **István Ilisz:** Conceptualization, Writing– Original Draft, Review & Editing; Supervision, Project Administration, Funding Acquisition

## Supplementary materials

Supplementary material associated with this article can be found, in the online version, at doi:10.1016/j.chroma.2021.462383.

## References

- [1] D.F. Hook, F. Gessier, C. Noti, P. Kast, D. Seebach, Probing the proteolytic stability of  $\beta$ -peptides containing  $\alpha$ -fluoro- and  $\alpha$ -hydroxy- $\beta$ -amino acids, *Chem-BioChem* 5 (2004) 691–706, doi:10.1002/cbic.200300827.
- [2] M.I. Aguilar, A.W. Purcell, R. Devi, R. Lew, J. Rossjohn, A.I. Smith, P. Perlmutter,  $\beta$ -Amino acid-containing hybrid peptides – New opportunities in peptidomimetics, *Org. Biomol. Chem.* 5 (2007) 2884–2890 doi:10.1039/b708507 a.
- [3] K. Gach-Janczak, J. Pieklińska-Ciesielska, A. Adamska-Bartłomiejczyk, R. Perlikowska, R. Kruszyński, A. Kluczyk, J. Krzywik, J. Sukiennik, M.C. Cerlesie, G. Caloe, A. Wasilewski, M. Zielińska, A. Janecka, Synthesis and activity of opioid peptidomimetics with  $\beta$ 2- and  $\beta$ 3-amino acids, *Peptides* 95 (2017) 116–123, doi:10.1016/j.peptides.2017.07.015.
- [4] K.H.Y. Duong, V.G. Góz, I. Pintér, A. Percel, Synthesis of chimera oligopeptide including furanoid  $\beta$ -sugar amino acid derivatives with free OHs: mild but successful removal of the 1,2-O-isopropylidene from the building block, *Amino Acids* 53 (2021) 281–294, doi:10.1007/s00726-020-02923-3.
- [5] G. Lelais, D. Seebach,  $\beta$ 2-amino acids-syntheses, occurrence in natural products, and components of  $\beta$ -peptides, *Biopolymers* 76 (2004) 206–243, doi:10.1002/bip.20088.
- [6] I. Ilisz, A. Bajtai, W. Lindner, A. Péter, Liquid chromatographic enantiomer separations applying chiral ion-exchangers based on Cinchona alkaloids, *J. Pharm. Biomed. Anal.* 159 (2018) 127–152, doi:10.1016/j.jpba.2018.06.045.
- [7] G. Lajkó, T. Orosz, N. Grecsó, B. Fekete, M. Palkó, F. Fülöp, W. Lindner, A. Péter, I. Ilisz, High-performance liquid chromatographic enantioseparation of cyclic  $\beta$ -aminohydroxamic acids on zwitterionic chiral stationary phases based on Cinchona alkaloids, *Anal. Chim. Acta.* 921 (2016) 84–94, doi:10.1016/j.aca.2016.03.044.
- [8] R. Sardella, F. Ianni, A. Lisanti, S. Scorzoni, F. Marini, S. Sternativo, B. Natalini, Direct chromatographic enantioresolution of fully constrained  $\beta$ -amino acids: exploring the use of high-molecular-weight chiral selectors, *Amino Acids* 46 (2014) 1235–1242, doi:10.1007/s00726-014-1683-5.
- [9] R. Berkecz, I. Ilisz, A. Misicka, D. Tymecka, F. Fülöp, H.J. Choi, M.H. Hyun, A. Péter, HPLC enantioseparation of  $\beta$ 2-homoamino acids using crown ether-based chiral stationary phase, *J. Sep. Sci.* 32 (2009) 981–987, doi:10.1002/jssc.200800561.
- [10] I. Ilisz, Z. Pataj, R. Berkecz, A. Misicka, D. Tymecka, F. Fülöp, H.J. Choi, M.H. Hyun, A. Péter, High-performance liquid chromatographic enantioseparation of  $\beta$ 2-amino acids using a long-tethered (+)-(18-crown-6)-2,3,11,12-tetracarboxylic acid-based chiral stationary phase, *J. Chromatogr. A.* 1217 (2010) 1075–1082, doi:10.1016/j.chroma.2009.07.003.
- [11] Z. Pataj, I. Ilisz, R. Berkecz, A. Misicka, D. Tymecka, F. Fülöp, D.W. Armstrong, A. Péter, Comparison of performance of Chirobiotic T, T2 and TAG columns in the separation of  $\beta$ 2- and  $\beta$ 3-homoamino acids, *J. Sep. Sci.* 31 (2008) 3688–3697, doi:10.1002/jssc.200800388.
- [12] Z. Pataj, R. Berkecz, I. Ilisz, A. Misicka, D. Tymecka, F. Fülöp, D.W. Armstrong, A. Péter, High-performance liquid chromatographic chiral separation of  $\beta$ 2-homoamino acids, *Chirality* 21 (2009) 787–798, doi:10.1002/chir.20670.
- [13] I. Ilisz, N. Grecsó, A. Aranyi, P. Suchotin, D. Tymecka, B. Wilenska, A. Misicka, F. Fülöp, W. Lindner, A. Péter, Enantioseparation of  $\beta$ 2-amino acids on cinchona alkaloid-based zwitterionic chiral stationary phases. Structural and temperature effects, *J. Chromatogr. A.* 1334 (2014) 44–54, doi:10.1016/j.chroma.2014.01.075.
- [14] I. Ilisz, N. Grecsó, A. Misicka, D. Tymecka, L. Lázár, W. Lindner, A. Péter, Comparison of the separation performances of cinchona alkaloid-based zwitterionic stationary phases in the enantioseparation of  $\beta$ 2- and  $\beta$ 3-amino acids, *Molecules* 20 (2014) 70–87, doi:10.3390/molecules20010070.
- [15] G. Hellinghausen, D. Roy, J.T. Lee, Y. Wang, C.A. Weatherly, D.A. Lopez, K.A. Nguyen, J.D. Armstrong, D.W. Armstrong, Effective methodologies for enantiomeric separations of 150 pharmacology and toxicology related 1°, 2° and 3° amines with core-shell chiral stationary phases, *J. Pharm. Biomed. Anal.* 155 (2018) 70–81, doi:10.1016/j.jpba.2018.03.032.
- [16] D.C. Patel, Z.S. Breitbach, M.F. Wahab, C.L. Barhate, D.W. Armstrong, Gone in seconds: Praxis, performance, and peculiarities of ultrafast chiral liquid chromatography with superficially porous particles, *Anal. Chem.* 87 (2015) 9137–9148, doi:10.1021/acs.analchem.5b00715.
- [17] R.M. Wimalasinghe, Z.S. Breitbach, J.T. Lee, D.W. Armstrong, Separation of peptides on superficially porous particle-based macrocyclic glycopeptide liquid chromatography stationary phases: consideration of fast separations, *Anal. Bioanal. Chem.* 409 (2017) 2437–2447, doi:10.1007/s00216-017-0190-4.
- [18] G. Kučerová, J. Vozka, K. Kalíková, R. Geryk, D. Plectitá, T. Pajpanova, E. Tesařová, Enantioselective separation of unusual amino acids by high performance liquid chromatography, *Sep. Purif. Technol.* 119 (2013) 123–128, doi:10.1016/j.seppur.2013.09.010.
- [19] D. Roy, D.W. Armstrong, Fast super/subcritical fluid chromatographic enantioseparations on superficially porous particles bonded with broad selectivity chiral selectors relative to fully porous particles, *J. Chromatogr. A.* 360339 (2019) 1605, doi:10.1016/j.chroma.2019.06.060.
- [20] D. Folprechtová, O. Kozlov, D.W. Armstrong, M.G. Schmid, Kvetta Kalíková, E. Tesařová, Enantioselective potential of teicoplanin- and vancomycin-based superficially porous particles-packed columns for supercritical fluid chromatography, *J. Chromatogr. A.* 460867 (2020) 1612, doi:10.1016/j.chroma.2019.460687.
- [21] C.L. Barhate, M.F. Wahab, Z.S. Breitbach, D.S. Bell, D.W. Armstrong, High efficiency, narrow particle size distribution, sub-2  $\mu$ m based macrocyclic glycopeptide chiral stationary phases in HPLC and SFC, *Anal. Chim. Acta.* 898 (2015) 128–137, doi:10.1016/j.aca.2015.09.048.
- [22] O.H. Ismail, A. Ciogli, C. Villani, M. De Martino, M. Pierini, A. Cavazzini, D.S. Bell, F. Gasparri, Ultra-fast high-efficiency enantioseparations by means of a teicoplanin-based chiral stationary phase made on sub-2  $\mu$ m totally porous silica particles of narrow size distribution, *J. Chromatogr. A.* 1427 (2016) 55–68, doi:10.1016/j.chroma.2015.11.071.
- [23] O.H. Ismail, M. Antonelli, A. Ciogli, M. De Martino, M. Catani, C. Villani, A. Cavazzini, M. Ye, D.S. Bell, F. Gasparri, Direct analysis of chiral active pharmaceutical ingredients and their counter ions by ultra-high performance liquid chromatography with macrocyclic glycopeptide-based chiral stationary phases, *J. Chromatogr. A.* 1576 (2018) 42–50, doi:10.1016/j.chroma.2018.09.029.
- [24] D. Roy, M.F. Wahab, T.A. Berger, D.W. Armstrong, Ramifications and insights on the role of water in chiral sub/supercritical fluid chromatography, *Anal. Chem.* 91 (2019) 14672–14680, doi:10.1021/acs.analchem.9b03908.
- [25] D.C. Patel, Z.S. Breitbach, J.J. Yu, K.A. Nguyen, D.W. Armstrong, Quinine bonded to superficially porous particles for high-efficiency and ultrafast liquid and supercritical fluid chromatography, *Anal. Chim. Acta.* 963 (2017) 164–174, doi:10.1016/j.aca.2017.02.005.
- [26] D.C. Patel, M.F. Wahab, T.C. O'Haver, D.W. Armstrong, Separations at the speed of sensors, *Anal. Chem.* 90 (2018) 3349–3356, doi:10.1021/acs.analchem.7b04944.
- [27] S. Du, Y. Wang, C.A. Weatherly, K. Holden, D.W. Armstrong, Variations of L- and D-amino acid levels in the brain of wild-type and mutant mice lacking D-amino acid oxidase activity, *Anal. Bioanal. Chem.* 410 (2018) 2971–2979, doi:10.1007/s00216-018-0979-9.
- [28] K. Schmitt, U. Woiwode, M. Kohout, T. Zhang, W. Lindner, M. Lämmerhofer, Comparison of small size fully porous particles and superficially porous particles of chiral anion-exchange type stationary phases in ultra-high performance liquid chromatography: effect of particle and pore size on chromatographic efficiency and kinetic performance, *J. Chromatogr. A.* 1569 (2018) 149–159, doi:10.1016/j.chroma.2018.07.056.
- [29] U. Woiwode, S. Neubauer, W. Lindner, S. Buckenmaier, M. Lämmerhofer, Enantioselective multiple heart cut two-dimensional ultra-high-performance liquid chromatography method with a core-shell chiral stationary phase in the second dimension for analysis of all proteinogenic amino acids in a single run, *J. Chromatogr. A.* 1562 (2018) 69–77, doi:10.1016/j.chroma.2018.05.062.
- [30] U. Woiwode, R.J. Reischl, S. Buckenmaier, W. Lindner, M. Lämmerhofer, Imaging peptide and protein chirality via amino acid analysis by chiral  $\times$  chiral two-dimensional correlation liquid chromatography, *Anal. Chem.* 90 (2018) 7963–7971, doi:10.1021/acs.analchem.8b00676.
- [31] W. Kopaciewicz, M.A. Rounds, J. Fausnaugh, F.E. Regnier, Retention model for high-performance ion-exchange chromatography, *J. Chromatogr. A.* 266 (1983) 3–21, doi:10.1016/S0021-9673(01)90875-1.
- [32] C.V. Hoffmann, M. Lämmerhofer, W. Lindner, Novel strong cation-exchange type chiral stationary phase for the enantiomer separation of chiral amines by high-performance liquid chromatography, *J. Chromatogr. A.* 1161 (2007) 242–251, doi:10.1016/j.chroma.2007.05.092.
- [33] T. Orosz, N. Grecsó, G. Lajkó, Z. Szakonyi, F. Fülöp, D.W. Armstrong, I. Ilisz, A. Péter, Liquid chromatographic enantioseparation of carbocyclic  $\beta$ -amino acids possessing limonene skeleton on macrocyclic glycopeptide-based chiral stationary phases, *J. Pharm. Biomed. Anal.* 145 (2017) 119–126, doi:10.1016/j.jpba.2017.06.010.
- [34] A.Y. Meyer, Molecular mechanics and molecular shape. Part 4. Size, shape, and steric parameters, *J. Chem. Soc. Perkin Trans. 2.* (1986) 1567, doi:10.1039/p29860001567.
- [35] A. Berthod, X. Chen, J.P. Kullman, D.W. Armstrong, F. Gasparri, I. D'Acquarica, C. Villani, A. Carotti, Role of the carbohydrate moieties in chiral recognition on teicoplanin-based LC stationary phases, *Anal. Chem.* 72 (2000) 1767–1780 doi:10.1021/ac991004 t.
- [36] J.C. Giddings, Dynamics of chromatography, Part 1: Principles and theory, Marcel Dekker, Inc., 1965.
- [37] I. Halász, R. Endeke, J. Asshauer, Ultimate limits in high-pressure liquid chromatography, *J. Chromatogr. A.* 112 (1975) 37–60, doi:10.1016/S0021-9673(00)99941-2.

- [38] F. Gritti, M. Martin, G. Guiochon, Influence of viscous friction heating on the efficiency of columns operated under very high pressures, *Anal. Chem.* 81 (2009) 3365–3384, doi:[10.1021/ac802632x](https://doi.org/10.1021/ac802632x).
- [39] A. de Villiers, H. Lauer, R. Szucs, S. Goodall, P. Sandra, Influence of frictional heating on temperature gradients in ultra-high-pressure liquid chromatography on 2.1 mm I.D. columns, *J. Chromatogr. A.* 1113 (2006) 84–91, doi:[10.1016/j.chroma.2006.01.120](https://doi.org/10.1016/j.chroma.2006.01.120).
- [40] B. Koppenhoefer, E. Bayer, Chiral recognition in the resolution of enantiomers by GLC, *Chromatographia* 19 (1984) 123–130, doi:[10.1007/BF02687727](https://doi.org/10.1007/BF02687727).
- [41] R.E. Boehm, D.E. Martire, D.W. Armstrong, Theoretical considerations concerning the separation of enantiomeric solutes by liquid chromatography, *Anal. Chem.* 60 (1988) 522–528, doi:[10.1021/ac00157a006](https://doi.org/10.1021/ac00157a006).
- [42] S. Allenmark, V. Schurig, *Chromatography on chiral stationary phases*, *J. Mater. Chem.* 7 (1997) 1955–1963 doi:[10.1039/a702403g](https://doi.org/10.1039/a702403g).
- [43] T. Fornstedt, P. Sajonz, G. Guiochon, Thermodynamic study of an unusual chiral separation, *J. Am. Chem. Soc.* 119 (1997) 1254–1264, doi:[10.1021/ja9631458](https://doi.org/10.1021/ja9631458).
- [44] G. Götmar, T. Fornstedt, G. Guiochon, Apparent and true enantioselectivity in enantioseparations, *Chirality* 12 (2000) 558–564 doi:[10.1002/1520-636X\(2000\)12:7<558::AID-CHIR2>3.0.CO;2-2](https://doi.org/10.1002/1520-636X(2000)12:7<558::AID-CHIR2>3.0.CO;2-2).
- [45] A. Sepsey, É. Horváth, M. Catani, A. Felinger, The correctness of van 't Hoff plots in chiral and achiral chromatography, *J. Chromatogr. A.* 1611 (2020) 6–8, doi:[10.1016/j.chroma.2019.460594](https://doi.org/10.1016/j.chroma.2019.460594).
- [46] L.D. Asnin, M.V. Stepanova, Van't Hoff analysis in chiral chromatography, *J. Sep. Sci.* 41 (2018) 1319–1337, doi:[10.1002/jssc.201701264](https://doi.org/10.1002/jssc.201701264).
- [47] E.N. Reshetova, M.V. Kopchenova, S.E. Vozisov, A.N. Vasyanin, L.D. Asnin, Enantioselective retention mechanisms of dipeptides on antibiotic-based chiral stationary phases: Leucyl-leucine, glycyl-leucine, and leucyl-glycine as case studies, *J. Chromatogr. A.* 1602 (2019) 368–377, doi:[10.1016/j.chroma.2019.06.025](https://doi.org/10.1016/j.chroma.2019.06.025).
- [48] L.D. Asnin, M.V. Kopchenova, S.E. Vozisov, M.A. Klochkova, Y.A. Klimova, Enantioselective retention mechanisms of dipeptides on antibiotic-based chiral stationary phases. II. Effect of the methanol content in the mobile phase, *J. Chromatogr. A.* 1626 (2020) 461371, doi:[10.1016/j.chroma.2020.461371](https://doi.org/10.1016/j.chroma.2020.461371).